# Low-temperature calorimetric properties of zinc ferrite nanoparticles

J. C. Ho
*Department of Physics, Wichita State University, Wichita, Kansas 67260*
*and National Institute for Aviation Research, Wichita State University, Wichita, Kansas 67260*

H. H. Hamdeh
*Department of Physics, Wichita State University, Wichita, Kansas 67260*

Y. Y. Chen, S. H. Lin, and Y. D. Yao
*Institute of Physics, Academia Sinica, Taipei, Taiwan*

R. J. Willey
*Department of Chemical Engineering, Northeastern University, Boston, Massachusetts 02115*

S. A. Oliver
*Center for Electromagnetics Research, Northeastern University, Boston, Massachusetts 02115*
(Received 20 March 1995)

Calorimetric measurements between 1 and 40 K by a thermal relaxation technique have been made on zinc ferrite nanoparticles prepared from an aerogel process. The expected λ-type heat-capacity peak near 10 K, which corresponds to a long-range antiferromagnetic transition in the bulk form of this material, is greatly suppressed. Broad peaks begin to prevail after the sample is annealed at 500 or 800 °C, but ball milling of the nanoparticles leads to almost complete disappearance of the low-temperature ordering. In all cases, calorimetrically based magnetic entropy at 40 K accounts for only a fraction of $2R\ \ln(2S+1)$ with $S=\frac{5}{2}$ for $Fe^{3+}$. These results are corroborated by magnetic data, which also indicate magnetic ordering at high temperatures. Such observations can be understood by considering the relative distribution of $Fe^{3+}$ between two nonequivalent (*A* and *B*) sites in the spinel-type lattice. In particular, the as-prepared fine particles show large $Fe^{3+}$ occupancy of the *A* sites, whereas these ions prefer the *B* sites in bulk zinc ferrite. Meanwhile, the lattice heat capacity is enhanced, yielding effective Debye temperatures of 225, 285, 345, and 360 K for the as-prepared, 500 °C-annealed, 800 °C-annealed, and ball milled sample, respectively, in contrast to 425 K for the bulk material.

## INTRODUCTION

Nanoparticles science and technology have been generating extensive interest in recent years in many research areas.[1,2] Rather different physical and chemical properties are observed from those of bulk materials. This study deals with a special case in zinc ferrite.

Ferrites have the general formula $(M_{1-c}Fe_c)[M_cFe_{2-c}]O_4$. The divalent metal element *M* (e.g., Zn, Mg, Mn, Fe, Co, Ni, or a mixture of them) can occupy either tetrahedral (*A*) or octahedral (*B*) sites of a spinel ($MgAl_2O_4$) structure as depicted by the parentheses ore brackets, respectively. The inversion parameter *c* is a measure of the fraction of $Fe^{3+}$ at *A* sites. Ferrimagnetic behavior often prevails as the result of strong interactions between magnetic sublattices occupying the *A* and *B* sites. Couple with their high magnetic permeability, high electrical resistivity, and low fabrication cost, many ferrites have been used for a long time in various electronic components.[3] In this context, while zinc is a common ingredient in technologically important mixed ferrites such as $Mn_{1-x}Zn_xFe_2O_4$ or $Ni_{1-x}Zn_xFe_2O_4$, pure zinc ferrite with $c\approx 0$ is basically paramagnetic at ambient temperatures. Nevertheless, it provides a simpler system to study the *B-B*-type magnetic interactions. Indeed, this compound was the subject of several earlier studies.

Earlier calorimetric measurements by Friedberg and Burk[4] resulted in a broad heat-capacity peak near 10 K, but the associated entropy was much smaller than $2R\ \ln 6$ as expected for a magnetic ordering of 2 moles of $Fe^{3+}$ with $S=\frac{5}{2}$ in each mole of $ZnFe_2O_4$ (241.07 g/mol). Questions were raised as to whether the ordering was long range in nature. The uncertainty was removed later though a λ-type heat-capacity anomaly observed by Westrum and Grimes.[5] Meanwhile, neutron diffraction[6,7] also revealed the superexchange induced antiferromagnetic ordering among $Fe^{3+}$ ions.

This report describes low-temperature calorimetric properties of zinc ferrite in the form of nanoparticles with a relative large inversion parameter. Magnetic behavior of similar materials have been reported recently by Sato *et al.*[8] and Kamiyama *et al.*[9] While their samples were synthesized by a coprecipitation method, the fine powders used in this work were prepared by an aerogel (supercritical sol-gel) technique. They were then either annealed at elevated temperatures to gradually

0163-1829/95/52(14)/10122(5)/$06.00  ©1995 The American Physical Society

reduce the inverse parameter, or ball milled to further promote disorder. In addition to the magnetic characterization, the calorimetric results also provide information on lattice contribution to heat capacity in these nanoscaled materials.

## EXPERIMENT

For samples preparation, zinc acetate dihydrate and ferric acetylacetonate, in 1:2 molar ratio, were first dissolved in a methanol/water mixture and sealed inside a stainless steel autoclave with a Pyrex liner. All ingredients other than the triply distilled water were obtained from Aldrich Chemical Company. The autoclave was heated at the rate of 2–3 °C/min to 250 °C, and the pressure reached 1700 psi (gauge). These conditions were above the critical point for methanol [$T_c = 239.5$ °C, $P_c = 1160$ psi (gauge)]. After the pressure was relieved at a constant temperature of 248 °C over a period of approximately 14 min, a slow flow of nitrogen gas was introduced into the autoclave while cooling overnight. The aerogel products were dark colored powders having essentially the same x-ray-diffraction pattern as that of $ZnFe_2O_4$ (Franklinite JCDPS No. 22-1012). The crystallite size $t$ was estimated from the Scherrer's method to be 8.1 nm, and the inversion parameter $c = 0.205$ was obtained using the Rietveld refinement. The lattice parameter was equal to 0.8450 nm, slightly larger than that of normal zinc ferrite. Transmission electron micrographs showed that the easily dispersible powders were fairly homogeneous with an average particle diameter near 14 nm. The fact that this is larger than 8.1 nm could be a consequence of the highly nonequilibrium nature of the aerogel process. While the x-ray-diffraction pattern is a signature of crystallites, overall particles may very well contain certain structurally disordered or even amorphous regions. In this regard, work is in progress to analyze a set of Mössbauer spectroscopic data on the same batch of sample materials. Part of the as-prepared zinc ferrite was then annealed as loose powders for 2 h in air at 500 or 800 °C, respectively, causing an increase in the crystallite size to 18.9 and 39 nm. However, reductions of the aerogel process-induced inversion and the structural disorder were the main results expected in the red or light brown products. Another portion was milled with tungsten carbide vial and balls for 10 h. Not surprisingly, x-ray diffraction yielded an enhanced $c = 0.55$ and $t = 10.3$ nm. No change occurred in the lattice parameter, but an amorphous phase was detected. Transmission electron micrographs showed a heterogeneous mixture of dispersible particles having mean dimensions of 40 nm and large agglomerations of smaller particles.

Heat-capacity measurements between 1 and 40 K were made on the as-prepared, 500 and 800 °C-annealed, and ball-milled samples using a thermal-relaxation microcalorimeter in a $^3$He cryostat. Each mg-size sample was prepared by lightly pressing the powders together without binder. It was thermally anchored with $\approx 50$ microgram grease to a sapphire holder on which thin films of germanium and nickel-chromium alloy were deposited to serve as temperature sensor and joule heating element, respectively. Temperature scale was based on a precalibrated germanium thermometer. The holder was thermally linked by four Au-Cu alloy wires to a temperature-regulated copper block. Following each heat pulse, the sample temperature relaxation rate was monitored to yield the time constant $\tau$. The heat capacity value was then calculated from $C = k\tau$, where $k$ is the thermal conductance of the Au-Cu wires. The heat capacity of the sample holder was separately measured for addenda correction. Overall uncertainties in the final results were within a few percent judging from the measurements of a copper standard.

Complementary magnetic measurements between 4 and 300 K were made using a superconducting quantum interference device. The applied field of 1000 G was below the saturation level at 10 K. Each sample had a mass of 10–40 mg.

## RESULTS AND DISCUSSION

There have been many publications concerning the particle size effect on heat capacity of solids, but most of which are metallic in nature. Therefore, discussions center around mainly the electronic and lattice term.[10] For insulting ferrites, the total heat capacity in Fig. 1 represents the sum of a lattice and a magnetic contribution instead. Also included in Fig. 1 for reference are literature data[5] for bulk $ZnFe_2O_4$ with inversion parameter $c \approx 0$. With the lattice contribution forming the background, a $\lambda$-type anomaly near $T_N \approx 10$ K reflects the long-range antiferromagnetic ordering among $Fe^{3+}$ ions in the $B$ sites of the normal spinel structure. Such a well defined character seems to be much reduced in the as-appeared fine powders, and broad peaks gradually emerge only following the 500 and 800 °C annealing. Ball milling

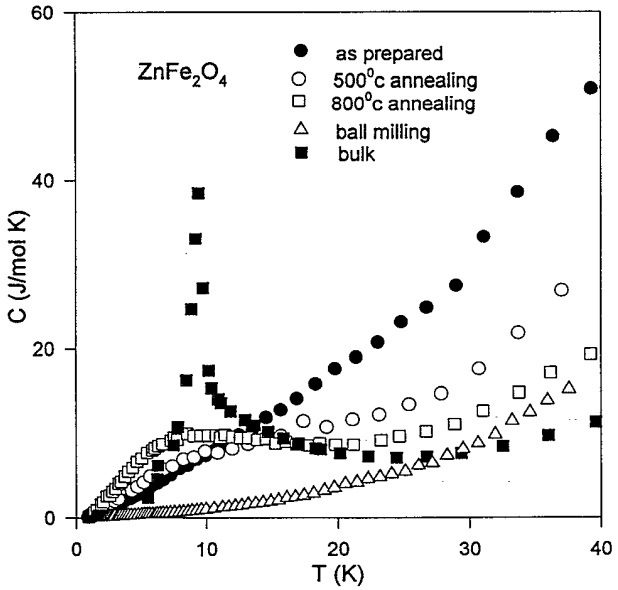


FIG. 1. Temperature dependence of heat capacity. All data from this work except those for the bulk zinc ferrite from Ref. 5.

TABLE I. Calculated Debye temperature of zinc ferrite from the Debye function. The heat-capacity value at 40 K is used as the fitting parameter, assuming $C \approx C_L$ with the magnetic contribution being negligible at this temperature.

| | $C$ at 40 K (J/mol K) | $\theta_D$ (K) |
|---|---|---|
| As prepared | 53 | 225 |
| 500 °C annealing | 32 | 285 |
| 800 °C annealing | 20 | 345 |
| Ball milling | 17.8 | 360 |
| Bulk (Ref. 5) | 11.1 | 425 |

leads to an opposite effect. Meanwhile, the lattice contribution to heat capacity appears to become enhanced in all cases. A better illustration in this regard can be found in Fig. 2 showing the temperature dependence of $C/T$. Indeed, a certain degree of magnetic ordering is revealed in the as-prepared sample. Such a data-plot format is also preferable in order to generate the magnetic entropy $S_m = \int (C_m/T) dT$ from the magnetic component of the total heat capacity. Questions arise as how to delineate $C_m$ from the lattice term $C_L$ in the total heat capacity. The following scheme to first estimate $C_L$ is employed to achieve this end.

One of the basis for this approach is the assumption that $C_m$ is negligibly small near the high-temperature end of measurements. This is justified since *A-B* coupling occurs at considerably higher temperatures, while antiferromagnetic *B-B* ordering is to a great extent confined to near 10 K or up to about 30 K as suggested by Fig. 2. This leads to the assignment of the total heat capacity values at 40 K, which are listed in Table I from extrapolation of actual data, to simply $C_L$ as upper limits. Nanoparticles have large fractions of atoms located on surface. It should be necessary to consider both two-dimensional (2D) and 3D vibrational modes. The 2D heat-capacity term would be more important at the lower temperature end of measurements,[11] but then it would become negligibly small relative to $C_m$ in this case. A second basis for the simplified analysis is, therefore, to assume that an effective 3D description is an acceptable approximation at 40 K. Using the 40-K heat capacity as fitting parameter in the standard Debye model analysis,[12] effective Debye temperatures $\theta_D$, also listed in Table I, are generated for the as-prepared, 500 °C-annealing, 800 °C-annealing, ball milling, as well as bulk zinc ferrite. Considering the

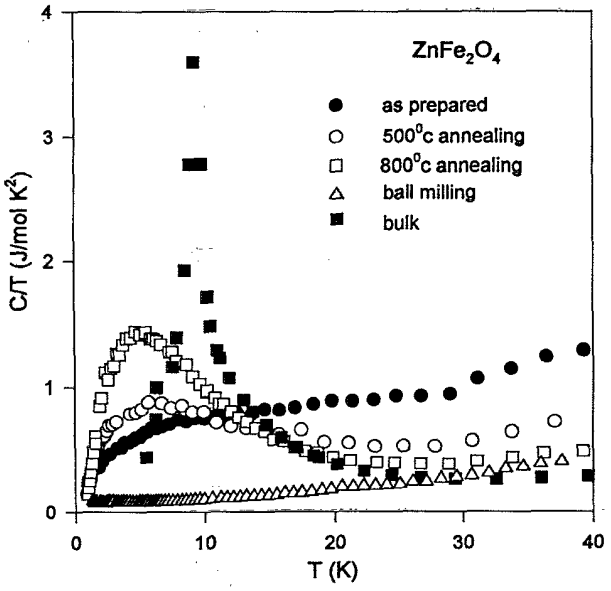


FIG. 2. Temperature dependence of $C/T$.

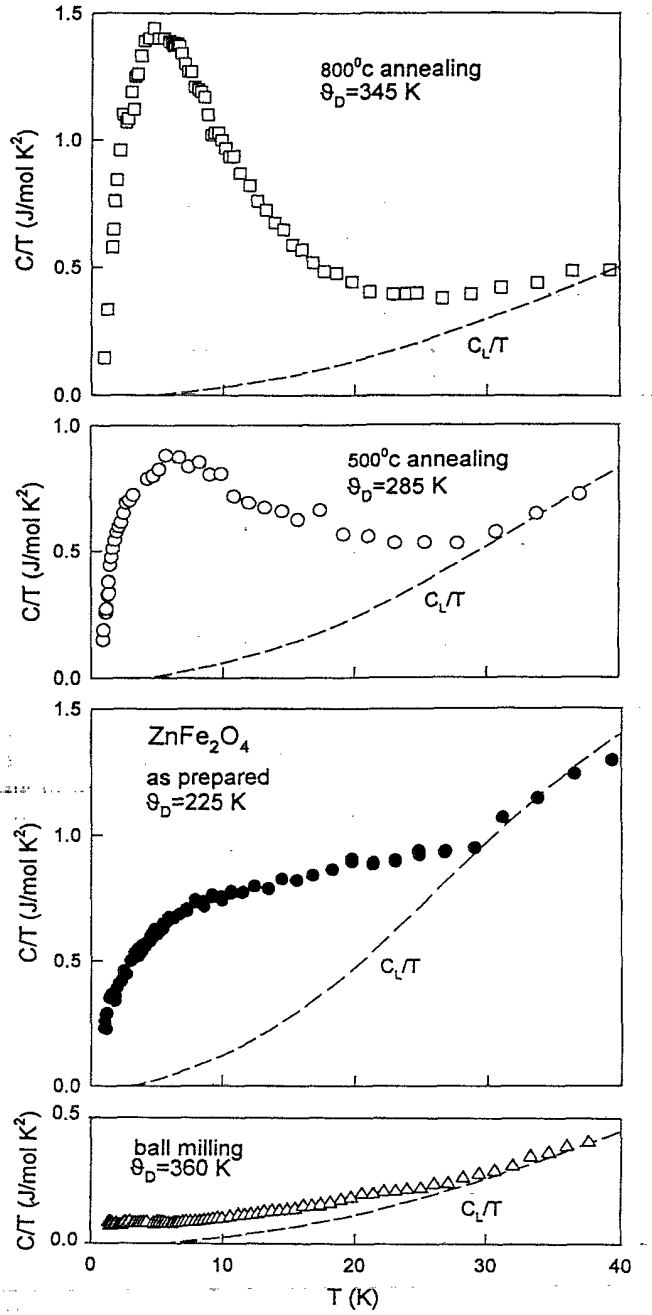


FIG. 3. Determination of lattice heat capacity by the Debye function, with the heat-capacity value at 40 K as the fitting parameter.

various assumptions involved here and the temperature dependence of effective $\theta_D$ in most solids, they should be viewed only as practical lower-limit parameters for comparison purposes. Nevertheless, the trend appears to be reasonable and the reduction in $\theta_D$ between bulk material and as-prepared nanoparticles can be deemed significant. The weaker bonding of large fractions of atoms located at the surface could be the major cause. The nonequilibrium condition in the as-prepared sample can also contribute to the lowering of $\theta_D$. The degree of disorder and the effective particle surface areas should diminish following thermal annealing, raising $\theta_D$ as observed. For the ball milled sample, agglomerations of still rather small sized particles may be the reason for the further reduction in $\theta_D$. Each $\theta_D$ value corresponds to a full range $C_L/T$ cure in Fig. 3. The difference plot yields $C_m/T=(C-C_L)/T$ in Fig. 4. Figure 5 shows the subsequently derived magnetic entropy through integration. The as-prepared sample has an $S_m$ value at 40 K approximately equivalent to only 40% of $2R$ ln6=30 J/mol K. Ball milling reduces it further, in contrast to the heat treatment effect. It should be noted that $S_m \approx 18$ J/mol K following the 800 °C annealing could still be underestimated as a consequence of the uncertainty in conjunction with the overassignment of lattice contribution to the total heat capacity.

These results on magnetic heat capacity can be understood considering the relative distribution of $Fe^{3+}$ ions at $A$ or $B$ sites. In the as-prepared condition with an inversion parameter of 0.205, much of the sample is already magnetically ordered through $A$-$B$ coupling at high temperatures, leaving only small portions to undergo the $B$-$B$ ordering at low temperatures.

Broad peaks in heat capacity gradually emerge following the 500 and 800 °C annealing, which significantly diminishes the inversion parameter. However, as pointed out earlier by Westrum and Grimes,[5] short-range ordering persists to much higher temperatures even in their otherwise well behaved bulk material. Apparently, zinc ferrites can hardly be totally inversion free. For a very small $c$, localized superparamagnetic clusters of low ordering temperatures are formed. This has been clearly

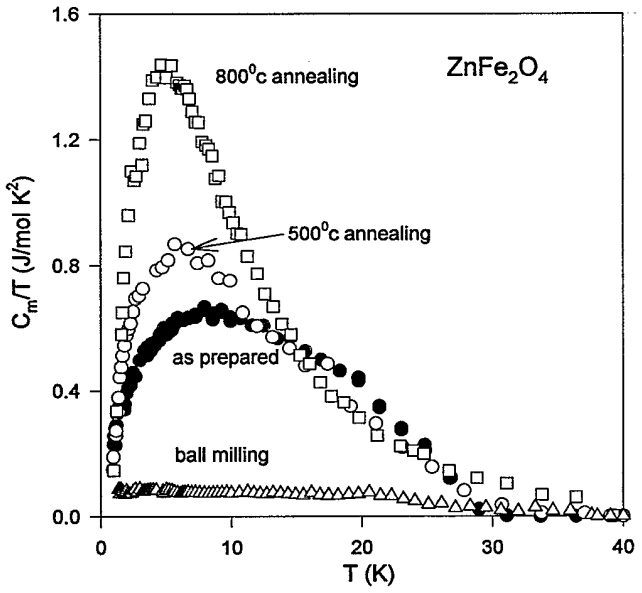


FIG. 4. Temperature dependence of $C_m/T=(C-C_L)/T$.

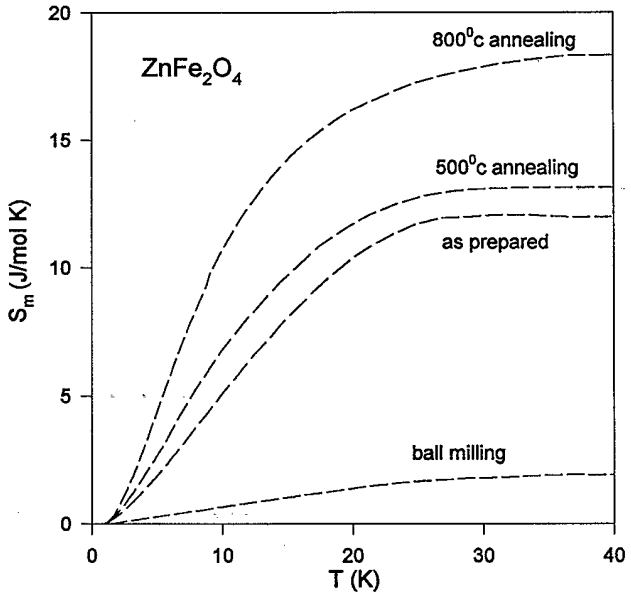


FIG. 5. Temperature dependence of magnetic entropy as derived from $S_m=\int (C_m/T)dT$. In comparison, $S_m=2R$ ln6=30 J/mol K if all $Fe^{3+}$ become fully ordered.

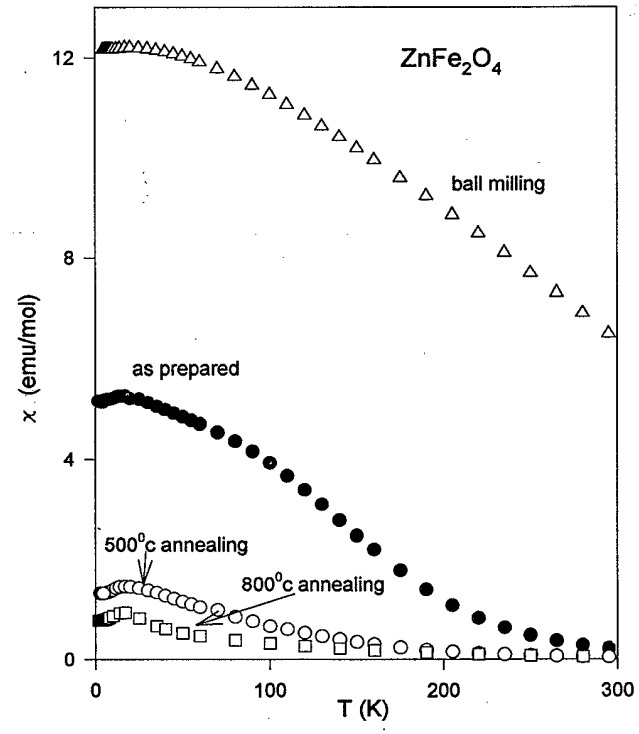


FIG. 6. Temperature dependence of magnetic susceptibility showing the onset of antiferromagnetic ordering at low temperatures. For the two thermally annealed samples, $d\chi/dT$ have maxima near $T_N \approx 10$ K.

observed by Mössbauer measurements. Because these clusters are heterogeneous, a spread in the ordering temperatures may account for the observed peak broadening. Superparamagnetism also tends to cause some broadening at the ordering temperatures. Moreover, although broad peaks were observed in bulk materials,[4] surface effects could not be ruled out in the fine particles system. As $c$ increases the material makes the transition to ferrimagnetism through complex magnetic states.

For the ball milled powder sample with an inversion parameter of about 0.6, the Mössbauer study shows ferrimagnetic order at room temperature. Consequently, the magnetic entropy associated with the low-temperature antiferromagnetic ordering almost completely disappears.

These calorimetric observations are also substantiated by magnetic susceptibility $\chi$ data in Fig. 6. First, $\chi$ decreases from the as-prepared to thermal annealed conditions, but the opposite occurs after ball milling. Clearly, the ferrimagnetic component in the material is proportional to the inversion parameter as expected. Secondly, a low-temperature ordering process is evident in the as-prepared and thermal-annealed samples, but barely seen in the ball milled one. The fact that the temperature dependence of $\chi$ exhibits a peak is a confirmation of the antiferromagnetic nature of the transition. Furthermore, the two thermal-annealed samples with better defined peaks yield maxima in $d\chi/dT$ near 10 K, in agreement with the heat-capacity data. however, the antiferromagnetic ordering effect is clearly a small component riding on a much larger ferrimagnetic susceptibility. In addition to the temperature dependence of the $A$- and $B$-sublattice magnetization and the $A$-$B$ interaction, the heterogeneous nature of the samples as well as the formation of superparamagnetic clusters add extra complications. Hopefully, the parallel program based on Mössbauer spectroscopic measurements in progress will be able to provide some insight in these respects.

## CONCLUSION

An aerogel process with subsequent thermal annealing or ball milling provide fine particles of zinc ferrite with very different inversion parameters $c$ of the spinel type structure. Part of each sample undergoes a broad antiferromagnetic transition near 10 K, revealed by both heat-capacity and magnetic susceptibility data. Calorimetrically determined entropy shows that the fraction of a given sample undergoing this $B$-$B$-type interaction-induced magnetic ordering decreases as $c$ increases. Meanwhile, the lattice heat capacity of the fine particles is every much enhanced, resulting in effective Debye temperature $\theta_D$ values ranging from 225 K for the as-prepared nanoparticles to 425 K for the bulk material.

## ACKNOWLEDGMENTS

This work was funded partially by NSF Grant No. OSR-955223 and National Science Council of the Republic of China Grant No. NSC82-0208-M-001-148. The crystallite size from x-ray diffraction by M. Daturi of the Istituto di Chimica, Università di Genova, Italy is gratefully acknowledged.

[1]R. W. Siegel, Phys. Today **46**, 64 (1993).
[2]H. Gleiter, Prog. Mater. Sci. **33**, 223 (1989).
[3]See, e.g., a review article by P. I. Slick, in *Ferromagnetic Materials,* edited by E. P. Wohlfarth (North-Holland, Amsterdam, 1980), Vol. 2, pp. 189–241.
[4]S. A. Friedberg and D. L. Burk, Phys. Rev. **98**, 1200 (1955).
[5]E. F. Westrum, Jr. and D. M. Grimes, J. Phys. Chem. Solids **3**, 44 (1957).
[6]J. M. Hastings and L. M. Corliss, Phys. Rev. **102**, 1460 (1956).
[7]U. König, E.F. Bertaut, Y. Gros, and G. Chol, J. Phys. (Paris) Colloq. **32**, C1-321 (1971).
[8]T. Sato, K. Haneda, M. Seki, and T. Iijima, Appl. Phys. A **50**, 13 (1990).
[9]T. Kamiyama, K. Haneda, T. Sato, S. Ikeda, and H. Asano, Solid State Commun. **81**, 563 (1992).
[10]See the review article by W. P. Halperin, Rev. Mod. Phys. **58**, 533 (1986).
[11]Y. Y. Chen, Y. D. Yao, B. T. Lin, S. G. Shyu, and H. M. Lin, Chin. J. Phys. **32**, 479 (1994).
[12]E. S. R. Gopal, *Specific Heats at Low Temperatures* (Plenum, New York, 1966), Appendix D.